Action Potential Propagation Through Tissue Lacking Gap Junctions: Application to Engrafted Cells in Myocardial Infarcts

Niels F Otani

Cornell University, Ithaca, NY, USA

Abstract

Engraftment of viable, electrically functional cells into a myocardial infarct as a method for restoring functionality is currently a topic of active research interest. Cells implanted in this way can form gap junction connectivity with each other, but often do not connect well with the surrounding tissue outside the infarct. Using a bidomain computer simulation model, we find that activation of these implanted cells by outside propagating action potentials is nevertheless possible, even if no gap junction connectivity to the surrounding tissue exists at all. The mechanism by which this action potential "tunneling" process occurs involves a current path that passes through both the intracellular and extracellular spaces, and is fundamentally spatially two-dimensional in nature. The typically convex boundary of the region occupied by these cells is found to greatly enhance the tunneling process, but unfortunately also hinders the ability of the activation of these cells to terminate reentrant waves propagating around the infarct.

1. Introduction

Recently, W. Roell et al. [1] demonstrated that action potential propagation could be induced in tissue engrafted into an infracted region of a mouse heart by action potentials traveling in the surrounding tissue, even though the latter was separated from the former by a region that was totally devoid of gap junctions. We will refer to this process as action potential "tunneling," a term borrowed from quantum mechanics, because it involves the propagation of a wave across a "forbidden" zone, only to continue propagating on the other side. In this preliminary study, we provide an explanation for how this could happen for the case of action potentials. The mechanism is essentially the same as one described by Barr & Plonsey [2] for two parallel fibers. Here we show how the mechanism extends to two spatial dimensions and then study the process in a simple geometry that is relevant to the case of engrafted, infarcted tissue.

2. Methods

The goal in this project was to study the fundamental properties and mechanism involved in action potential tunneling, so the computer simulations we conducted employed a simple Fitzhugh-Nagumo model of the ion channel dynamics, which was embedded into a standard bidomain model. The equations were thus,

$$\frac{\partial V_m}{\partial t} = \frac{1}{\epsilon_1}\left(V_m - \frac{V_m^3}{3} - W\right) + \nabla\cdot(\mathbf{D}_i\cdot\nabla(V_m+\phi_e)) \quad (1)$$

$$\frac{\partial W}{\partial t} = \epsilon_2(V_m - \gamma W + \beta) \quad (2)$$

$$\nabla\cdot((\mathbf{D}_i+\mathbf{D}_e)\cdot\nabla\phi_e) = -\nabla\cdot(\mathbf{D}_i\cdot\nabla V_m) \quad (3)$$

where V_m is the transmembrane potential, ϕ_e is the extracellular potential, and W is the standard Fitzhugh-Nagumo measure of refractoriness. All simulations were run with $\gamma = 0.8$ and both matrices $\mathbf{D}_i$ and $\mathbf{D}_e$ equal to diag(1.0,1.0). The extracellular potential field was found using the default sparse matrix inversion package within Matlab (Mathworks, Inc.), while the membrane potential and W were advanced in time using the forward Euler method with a timestep size of 1.25×10^{-3}. Early simulations were conducted on a 50x50 square grid, with a grid spacing $\Delta x = \Delta y = 0.2$ in each direction, with $\epsilon_1 = \epsilon_2 = 0.2$ and $\beta = 0.46$. These simulations were used to generate all the figures presented here except Fig. 3. For that figure, ϵ_1 was changed to 0.05, β varied as described below, and a finer, 100x100 square grid was employed, with grid spacings of $\Delta x = \Delta y = 0.1$.

3. Results

Linear barrier. We first ran simulations in a domain that contained a line-shaped region lacking gap junctions. This "linear barrier" was created by removing all gap junctions crossing a line that extended from bottom to top of the simulation domain, and was situated in the center of the system horizontally. When a plane-wave action potential was launched from the left edge, the wave exhibited the classically-expected behavior; namely, its propagation was

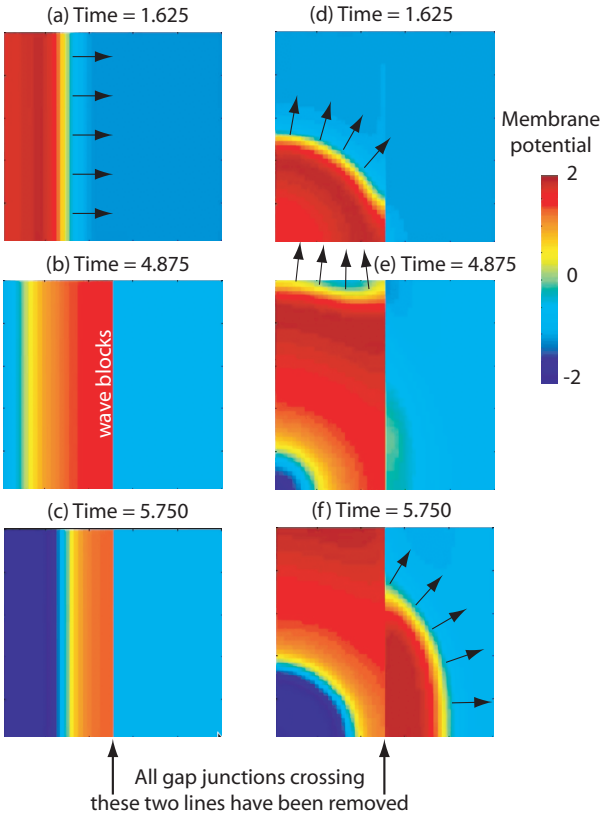

Figure 1. Snapshots taken at various times from two simulations having identical, vertically-oriented, line-shaped regions that contain no gap junctions. (a–c) Membrane potential (V_m) colorplots from the first simulation, which launches a plane wave action potential from the left edge. (d–f) Membrane potential colorplots for the second simulation, in which an action potential is launched from a small group of cells in the lower-left corner.

abruptly halted at the barrier, and no effect of the wave was visible on the other side (Figs. 1(a–c)). In contrast, when the wave was launched at the barrier from an angle, as in Figs. 1(d–f), we found that the wave caused a secondary region of depolarization to appear on the distal side of the barrier, as in Figs. 1(e & f), which then resulted in the propagation of a secondary wave. The total lack of response of cells on the right side of the barrier in the first simulation, when compared to the induction of a secondary wave in the second simulation, strongly suggests that the mechanism involved is inherently two-dimensional.

Circular barrier. We next looked at the case of a ring-shaped, gap-junctionless region. This configuration was intended to be a simple model of the engrafted, infarcted situation: The region inside the ring represents the engrafted cells, while the ring itself represents the gap between these cells and the surrounding, normal tissue. When a wave was launched at this barrier from the outside, we again obtained the delayed induction of a propagating action potential wave inside the barrier, as shown in Figs. 2(a–c). The implication is that it is in theory possible to induce a propagating wave in the engrafted cells, even if they have no gap junction connectivity whatsoever to the surrounding, normal tissue. We also found that it was possible for the induced wave to propagate in the direction opposite that of the primary wave (retrograde propagation). This happened most often when with the thicker barriers, as shown in Fig. 2(d–f).

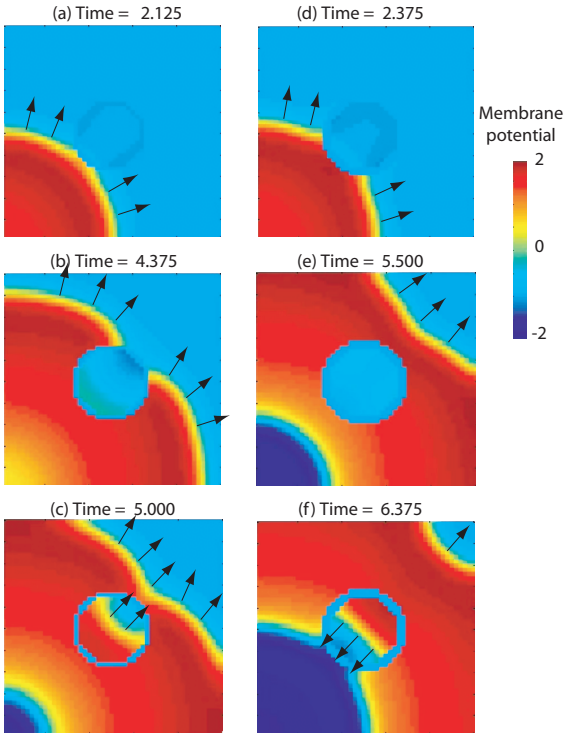

Figure 2. Membrane potential snapshots taken at various from two simulations containing a circular barrier: (a–c) The barrier with is 0.4, (d–f) The barrier width is 0.6.

Comparison of the linear and circular barrier configurations. To gain further insight into the action potential tunneling mechanism, we ran several additional simulations with both the linear and circular barrier configurations using different values of β and the barrier thickness. We expressed the latter in units of the space constant λ, which was found to be 0.1407, obtained by measuring the exponential falloff of V_m from a small bipolar, extracellular DC current source. The primary wave was initiated in the lower-left corner of the simulation domain in all cases. The results are shown for linear and circular barriers in Figs. 3(a) and (b), respectively.

The linear barrier simulations actually exhibited a number of different wave induction patterns. In order from the darkest to the lightest orange colors appearing in Fig. 3(a), we observed secondary wave induction just to the distal

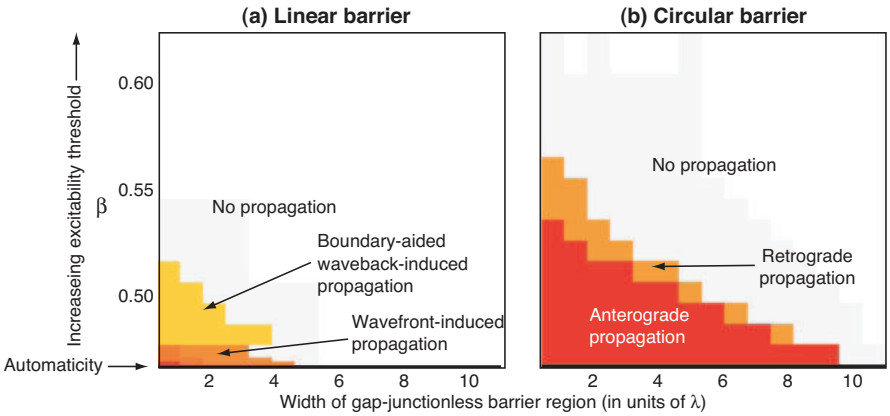

Figure 3. Type of wave induced in the region across the barrier as a function of two parameters: β and the width of the barrier, for the cases of (a) the linear barrier, and (b) the circular barrier.

side of the barrier (1) in the lower corner, (2) simultaneously in the lower corner and in the center, (3) just in the center, and (4) in the top corner. In the plot, we classified all of these as "wavefront-induced propagation." In a large number of cases, the leading edge of the primary did not induce wave propagation, but the trailing edge of the wave did. In these cases, the wave invariably originated from the top corner on the distal side of the barrier. Induction of this wave appeared to be aided by the favorable source-sink ratio created there by the presence of the no-flow boundary conditions imposed on the top edge. These cases are color-coded in yellow in Figs. 3(a), and are designated as "boundary-aided waveback-induced propagation."

Induction of the secondary wave was considerably easier when the barrier was circular. Figure 3(b) shows that wave induction inside the barrier in either the anterograde or retrograde directions occurred over a much larger region in parameter space that was the case for the linear barrier. This was presumably because a much more favorable source-sink relationship existed in this case—there were far fewer cells inside the ring than depolarized cells outside, due both to the small area inside the ring and the convex curvature of its circular boundary. We also note that, as in Fig. 2, induced retrograde propagation tended to occur for the larger barrier thicknesses, when anterograde propagation was not possible.

As expected, Figs. 3(a) and (b) both show that the ability of the primary wave to induce secondary wave propagation on the opposite side of the barrier decreases with increasing width of the barrier. Since the height of the excitability threshold increases with β, it is also not surprising that this ability increases with decreasing β. In fact when β is close to the value at which automaticity (i.e., spontaneous depolarization) starts (at $\beta = 0.463$), induction can take place across a very thick barrier—as wide as 9 space constants for the case of the circular barrier (Fig. 3(b)).

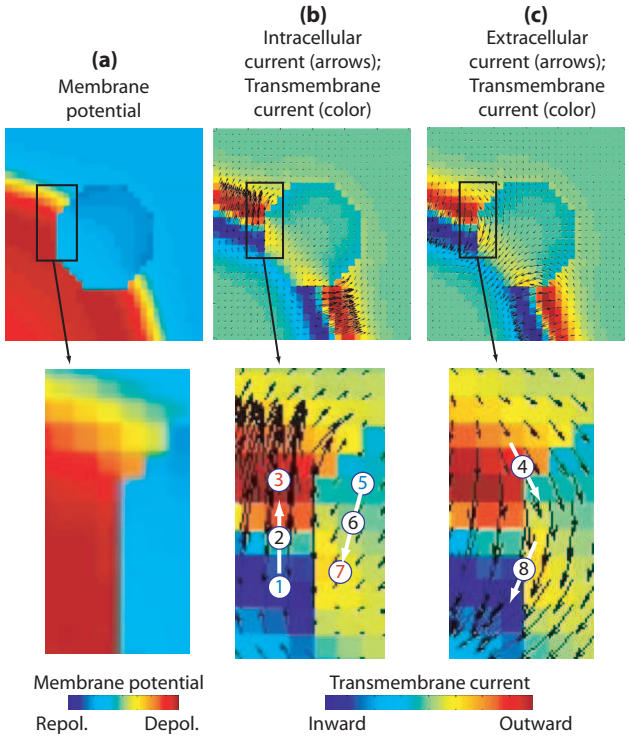

Figure 4. Three magnified views of the interaction of the primary action potential wavefront with the circular barrier and the region within.

The action potential tunneling mechanism. The mechanism by which wave propagation is induced is revealed by careful examination of the electrical current pattern that leads to depolarization on the other side of the barrier. Eight steps are involved, as depicted by the circled numbers in the pattern of electrical currents observed in the vicinity of the circular barrier (Fig. 4): (1) The inward (sodium) current responsible for the upstroke of the

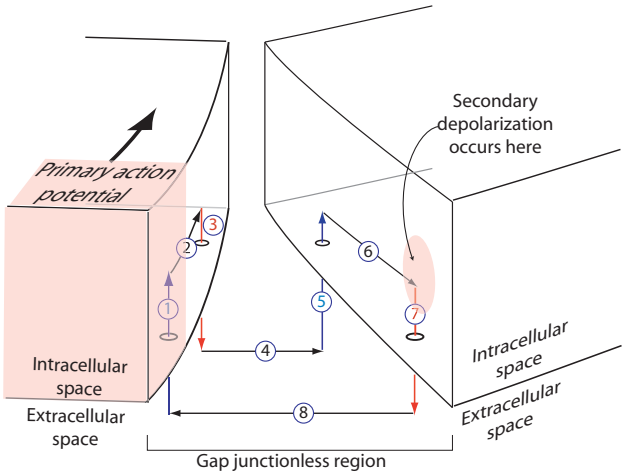

Figure 5. Schematic of the mechanism by which a propagating action potential on one side of a gap-junctionless barrier can induce depolarization and wave propagation on the other side.

primary wave is also the current source for the mechanism (blue color in Fig. 4(b)). (2) Current flows from this source through gap junctions ahead of the primary wave (upward arrows in Fig. 4(b)). (3) Current flows out through the membrane into the extracellular space (red regions in Figs. 4(b) and (c)). (4) Current flows across the gap-junctionless gap in the extracellular space. (5) Current re-enters the intracellular space (light-blue region in Figs. 4(b) and (c)). (6) Current flows intracellularly in the retrograde direction. (7) Current capacitively charges the membrane, causing depolarization (yellow-orange region in Fig. 4(b)). (8) Current flows back across the barrier, closing the loop. An action potential wave will be launched from location (7) if the depolarization produced by this mechanism is sufficient. A schematic diagram of these same eight steps is shown in Fig. 5.

Inability of the induced wave to stop a reentrant wave propagating around the infarct. When a reentrant wave is initiated that propagates around the circular barrier, we find that it readily and repeatedly launches waves inside the barrier. However, even with the thinnest possible barrier (equal to Δx), a very low excitability threshold ($\beta = 0.464$, only 0.001 above the automaticity value), and a very large barrier radius (28.4λ) so as to provide the most favorable source-sink relationship, we still find that these induced waves have no obvious effect back on the reentrant wave, and in particular do not stop its continued propagation.

4. Discussion and conclusions

This study shows that it is theoretically possible for action potential waves to cross regions that are totally lacking gap junctions. This tunneling process is possible because current generated by the primary wave can cross the barrier in the extracellular space, excite the tissue on the far side, and return across the barrier in a different location to complete the circuit. The circuit the current follows can therefore only exist in two or more spatial dimensions. A favorable source-sink relationship appears to strongly enhance the process, allow induction of action potentials to occur much more readily inside a circular barrier than across a line-shaped one. Unfortunately, the same strong dependence on the source-sink relationship also appears to prevent the induced wave inside a circular barrier from playing any role in terminating a reentrant wave propagating around the outside. Although action potential tunneling bears some similarity to the corresponding effect in the engrafted infarcted hearts, we currently have no reason to believe (or disbelieve) that this mechanism is responsible for the induced depolarization seen in these engrafting experiments. Additional simulations with more realistic ion channel models and geometry should be performed to check the validity of these results.

Acknowledgements

The author wishes to thank B. Roth, R. F. Gilmour, Jr., and M. I. Kotlikoff for advice and suggestions. This work was supported in part by by Award Number R01HL089271 from the National Heart, Lung, And Blood Institute. The content is solely the responsibility of the author and does not necessarily represent the official views of the National Heart, Lung, and Blood Institute or the National Institutes of Health.

References

[1] Roell W, Lewalter T, Sasse P, Tallini YN, Choi BR, Breitbach M, Doran R, Becher UM, Hwang SM, Bostani T, von Maltzahn J, Hofmann A, Reining S, Eiberger B, Gabris B, Pfeifer A, Welz A, Willecke K, Salama G, Schrickel JW, Kotlikoff MI, Fleischmann BK. Engraftment of connexin 43-expressing cells prevents post-infarct arrhythmia. Nature Dec 2007;450:819–824.

[2] Barr RC, Plonsey R. Electrophysiological interaction through the interstitial space between adjacent unmyelinated parallel fibers. Biophys J May 1992;61:1164–1175.

Address for correspondence:

Niels F. Otani
Department of Biomedical Sciences
Cornell University
Ithaca, New York 14853-6401, USA
nfo1@cornell.edu